Squeeze film damping in the free molecular region with full thermal accommodation

M.A.G. Suijlen[1,2], J.J. Koning[2], M.A.J. Van Gils[2], H.C.W. Beijerinck[1]
[1] Stan Ackermans Institute, Technical University Eindhoven, Netherlands,
[2]NXP Semiconductors, Innovation and Technology, Nijmegen, Netherlands

*Corresponding author: M.A.G. Suijlen, phone: +31(0)40 2729589, fax: +31(0)40 2743352, e-mail: matthijs.suijlen@nxp.com

Keywords: MEMS, squeeze film damping, free molecular flow

1. Introduction

In the study of the dynamic behaviour of MEMS devices, damping forces resulting from surrounding air generally play a significant role. As the most commonly used technologies are capacitive sensing and electrostatic driving, for which narrow air gaps often result, the so-called squeeze film effect dominates the interaction of the surrounding air with the moving part of a MEMS device. This effect refers to the pumping action of a fluid between closing up parallel surfaces with a gap much smaller than their dimensions. It exceeds the drag force on the MEMS part that would be experienced in isolated motion considerably. Current descriptions of squeeze film air damping are derived considering a continuum fluid picture of the flow in the squeeze film. In many MEMS, however, squeeze film flow cannot be regarded as continuum-like. Gases trapped in the MEMS cavity often are so rarefied that the molecular mean free path exceeds the gap dimensions and flow becomes 'free molecular'. In this regime, gas-gas collisions in the cavity are unimportant and momentum is transferred between gas and surface by ballistic trajectories and wall collisions. Thus the way to meaningfully describe the interaction of MEMS parts with the gas is to consider the sum of all individual wall collisions. Previously Bao et al. [1] used a ballistic approach to establish an analytical model for squeeze film damping of vibratory microstructures in the free molecular region. However, all wall collisions are treated as elastic collisions with specular (mirror like) reflection. The initial conditions determine the full trajectory, following a straight line when projected in the plane of the MEMS. The molecules are accelerated by each impact with the oscillating MEMS, resulting in the dissipation of mechanical energy of the MEMS, i.e., damping is introduced by the molecules propelled out of the gap by their straight-line motion. The model of Bao shows reasonable agreement with experimental observations of air damping on resonators with a beam-like geometry [2] with a large length-to-width ratio. We observe deviations up to a factor two from our observations on resonators with a plate-like geometry.

2. Random walk transport

To get rid of the rather unrealistic assumption of specular reflection of gas molecules on an industrially "clean" surface of the MEMS, we developed a new analytical model for squeeze film damping of MEMS resonators in the free molecular flow regime. Corner stone of this derivation is the assumption of so-called full thermal accommodation in molecule-wall interactions. This implies that, every time a molecule hits a wall, the molecule's state is lost and reset to a new random state distributed according to Maxwell-Boltzmann statistics. As a result, the molecules will perform a random walk in the cavity, bouncing up and down between microstructure and substrate and erratically zigzagging along its trajectory as projected in the plane of the device (Fig.1). In each collision with the MEMS, mechanical energy is transferred from the device to the molecule due to the moving coordinate frame that the MEMS represents. This energy is dissipated in the next collision with the substrate that serves as the other wall of the gap. Thus, kinetic energy of the microstructure is dissipated, which explains the damping force. Application of this idea arises from the extreme conditions (UHV and high temperature surface annealing) that are required to create specular reflection in the sophisticated practice of molecular beam experiments used to investigate the dynamics of molecule-surface collisions. Because such conditions are not available in the low-cost applications where MEMS devices are used, it is unrealistic to assume this type of molecule-wall interaction and full thermal accommodation of the molecules has to be included in models describing squeeze film damping in the regime of free molecular flow.

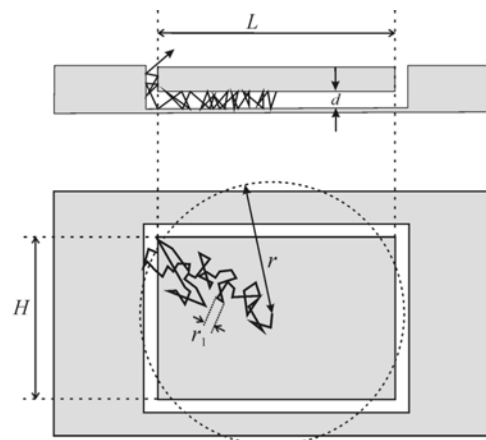

Figure 1: Random walk diffusion in a MEMS cavity

3. Squeeze film interaction

Since molecular transport with full thermal accommodation of the molecules is considerably slower than transport mediated by specular reflection, it takes considerably more time to equilibrate the density variations $\Delta n(t)$ of the gas as generated by the oscillatory displacement $z(t)$ of the membrane. The slow process of random walk diffusion then acts to cancel this density variation. The density variation $\Delta n(t)$ is governed by the differential equation :

$$\frac{d}{dt}\left(\frac{\Delta n}{n}\right) = -\frac{1}{\tau_d}\frac{\Delta n}{n} - \frac{d}{dt}\left(\frac{z}{d}\right), \qquad (1)$$

with τ_d the relaxation time, n the equilibrium value of the density, and z the coordinate pointing up from the membrane (Fig.1) with $z = 0$ corresponding to its equilibrium position. The equation describes the rate of change in density, as counteracted by the random walk diffusion (first term) and driven by the displacement z of the membrane (second term). Assuming a forced membrane oscillation with displacement $z = z_0\, e^{i\omega t}$ and a trial solution $\Delta n(t)/n = (\Delta n_0/n)\, e^{i\omega t}$ with complex amplitude, we find

$$\frac{\Delta n}{n} = -\frac{z}{d}\cdot\frac{i\omega\tau_d}{1+i\omega\tau_d} \qquad (2)$$

In case of isothermal density variations $\Delta n(t)$, the force exerted on the membrane is given by

$$F_{\text{memb}} = \Delta n(t)\ k_B\, T A, \qquad (3)$$

with A the frontal area of the moving membrane. Combining eqs. 2 and eq. 3 the squeeze force F_{squeeze} of the gas in the cavity on the moving membrane thus satisfies:

$$F_{\text{squeeze}} = -\frac{pA}{d}\cdot\frac{i\omega\tau_d}{1+i\omega\tau_d}\, z\ , \qquad (4)$$

consisting of a real and imaginary contribution. The real part raises the elastic force $-k\,z$ on the oscillating mass m of the MEMS; the imaginary part raises the damping force $-b\,\dot{z}$ according to the differential equation

$$m\,\ddot{z} + b\,\dot{z} + k\,z = F_0 e^{i\omega t} \qquad (5)$$

with

$$b = b_{\text{mat}} + b_{\text{squeeze}} \ \text{ and} \qquad (6)$$

$$k = k_{\text{mat}} + k_{\text{squeeze}} \qquad (7)$$

Here, b_{mat} and k_{mat} represent the inherent damping and stiffness of the mechanical structure. The contributions due to the complex valued squeeze force F_{squeeze} are given by:

$$b_{\text{squeeze}} = \frac{pA}{d}\frac{\tau_d}{1+(\omega\tau_d)^2} \qquad (8)$$

$$k_{\text{squeeze}} = \frac{pA}{d}\frac{(\omega\tau_d)^2}{1+(\omega\tau_d)^2} \qquad (9)$$

In a plot of these constants versus frequency ω, one can clearly see the character of the squeeze film interaction: for very slow oscillation, $\omega \ll 1/\tau_d$, it manifests itself as pure damping force and for fast oscillation, $\omega \gg 1/\tau_d$, it becomes an elastic force without damping.

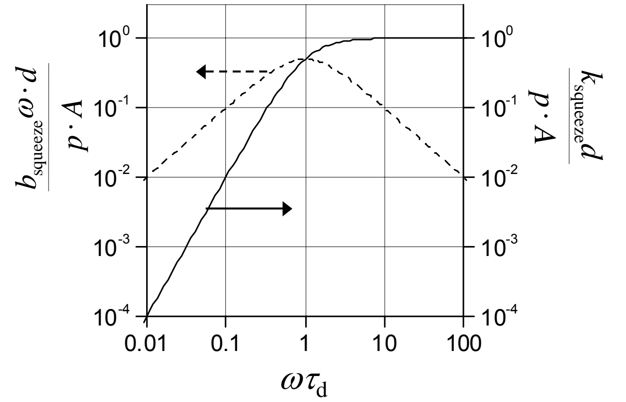

Figure 2: frequency characteristic of the squeeze film interaction.

These results show how we can optimize the design of MEMS resonators. E.g., for an application as a pressure sensor, we have to choose $\omega\tau_d = 1$ for maximum sensitivity. To avoid a shift in the operating frequency, we can choose $\omega\tau_d = 0.3$, with a slight trade-off in maximum sensitivity. Conversely, to use a frequency shift as pressure read-out instead of the change in quality factor, we can choose $\omega\tau_d > 3$ as range of operation.

4. Diffusion time

For calculation of the diffusion time τ_d consider the random walk of a molecule in a MEMS cavity like shown in fig 1. The average value of the squared distance $\langle r^2\rangle$ travelled by the molecule is related to the square of the average unit step $\langle r_1\rangle^2$ by

$$\langle r^2\rangle = N\langle r_1\rangle^2, \qquad (10)$$

with N the number of wall collisions. For a rectangular plate oscillator, the average squared distance to its circumference equals

$$\langle r^2\rangle = A/\pi \qquad (11)$$

as derived from a simple geometrical calculation. The average value of the unit step size equals $\langle r_1\rangle = \pi\cdot d/2$, which is obtained by averaging $r_1 = d$ tan

θ over the flux impinging on the wall using Maxwell Boltzmann statistics. The same approach results in $\tau_1 = 2\, d / \langle v \rangle$ with $\langle v \rangle = \sqrt{8 k_B T / (\pi \cdot m)}$ the average velocity of the gas molecules. Combining these results gives

$$\tau_d = N \cdot \tau_1 = \frac{8}{\pi^3} \frac{A}{d \langle v \rangle}. \qquad (12)$$

Now all information is available to compare the model predictions with our measurements for a solid resonator membrane. In our case however the resonator membranes are perforated to facilitate the wet etch during processing. These etch holes provide extra escape channels for the molecules from the gap and thus reduce the diffusion time τ_d drastically.

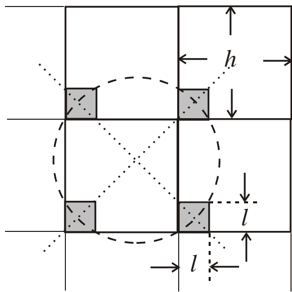

Figure 3: fragment of membrane with h x h sized unit cells provided with l x l sized etch holes

A simple geometrical model, taking into account only the first four etch holes surrounding the starting position of the molecule, results in a unit cell escape probability Γ given by

$$\Gamma = \frac{4}{\pi} \frac{l}{h} \qquad (13)$$

with *h* the unit cell size and *l* the etch hole size (Fig.3). Understanding a diffusing molecule will not escape until a certain number of holes *s* have passed, we can write the effective value $\tau_{d,eff}$ of the diffusion time as a power series in complementary probability $(1-\Gamma)$:

$$\tau_{d,eff} = \Gamma\ \tau_d\ (1 + 2\ (1-\Gamma) + 3\ (1-\Gamma)^2 + \ldots + s\ (1-\Gamma)^{s-1}) \qquad (14)$$

In the extreme case of an infinitely large device this series yields $\tau_{d,eff} = \tau_d / \Gamma$ with τ_d the diffusion time corresponding to a single unit cell. The series is correctly normalized by

$\Gamma_s = \Gamma + \Gamma\ (1-\Gamma) + \Gamma\ (1-\Gamma)^2 + \ldots + \Gamma\ (1-\Gamma)^s$ so that $\Gamma_\infty = 1$.

When Γ is large, a few terms of eq.(14) already suffice, as indicated by a partial escape probability $\Gamma_s \sim 1$. For our experiments, with $\Gamma = 0.46$, we find $\tau_d < \tau_{d,eff} < 2.2\,\tau_d$. Of course, this is a zeroth order result that has to be verified by Monte Carlo calculations.

5. Experiments

To test the model, we have investigated the pressure dependency of the damping coefficient of two different resonators. The devices consist of a rectangular plate supported by cantilever beams above the substrate (***figure 4***). The gaps between the support beams allow gas molecules to escape along the edges during the squeeze action of the plate. Characteristic data and dimensions of the devices are given in ***table 1***. The spring constant *k* is derived from a finite element simulation of the device using “COMSOL Multiphysics”. The devices are labelled ‘8x8’ and ‘8x2’, referring to their size in terms of a unit cell of 50 x 50 µm^2 apart from a 30 µm wide strip along the left vertical and upper horizontal edge.

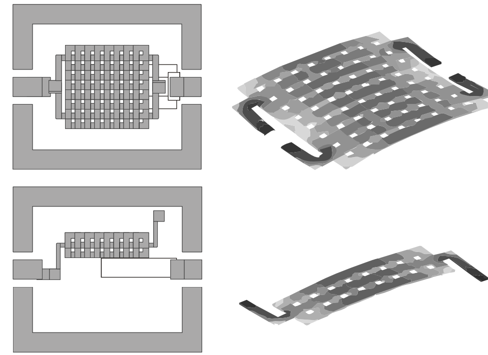

Figure 4: Design (left) and mode shape (right) of the MEMS resonator samples used to measure the air pressure dependency of the damping. The upper sample is referred to as ‘8x8’ and lower as ‘8x2’.

This movable, aluminium plate and substrate metallization form a variable capacitor. Plate motion was detected via capacitance changes measured using an HP4194 impedance analyser.

[P1]

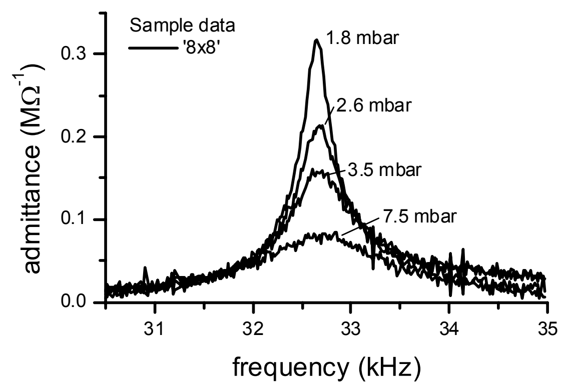

Figure 5: Admittance signal of the '8x8' sample for different pressures.

At resonance, the plate amplitude rises and more mechanical energy is dissipated in the ambient gas. Since this dissipated energy must be supplied

by the analyser, a peak is seen in the magnitude of the admittance. Typical experimental results are shown in ***figure 5***. For four different values of the ambient pressures in the test chamber, ranging from 1.8 to 7.5 mbar, the resonance signal of the 8x8 device is shown as a function of the generator frequency. We clearly see the decrease of the quality factor with increasing pressure. The shift of the resonance frequency due to the extra contribution k_{squeeze} is very small, indicating that we operate at $\omega\tau_{\mathrm{d}}$ << 1.

Table 1: Sample properties used for model evaluation. Frequency and spring constant as simulated by COMSOL

Device	8x8	8x2
Plate material	aluminium	aluminium
Plate thickness	4.5 μm	4.5 μm
Substrate gap width (*d*)	3.0 μm	3.0 μm
Etch hole fraction (l/h)	0.36	0.36
Plate area (*A*)	430 x 430 μm^2	430 x 130 μm^2
Frequency ($\omega_0/(2\pi)$)	37 kHz	36 kHz
Spring constant (k_{mat})	81 N/m	33 N/m

6. Results

By determining the quality factor Q of the resonance peaks (***figure 5***) we can calculate the damping coefficients of the resonators, using the relation $b = k/(\omega_0\ Q)$[P2]. Because $k_{\mathrm{squeeze}} << k_{\mathrm{mat}}$ we have only used the latter to calculate the damping coefficient b.

In ***figure 6*** we show the experimental results for the damping *b* as a function of the pressure in the test chamber at ambient temperature *T* = 22°C. Since the observed damping constants turn out to be many times larger than the (extrapolated) damping at 0 mbar, damping is squeeze force dominated hence b_{squeeze} can be taken directly from the total damping *b*. For both resonators we observe a good agreement of the model predictions with the experimental results, with the model results 50% larger than the experiments indicate (***table 2***).

Table 2: Summary of experimental results on two different MEMS resonators specified in fig. 4 and tab. 1.

Device	8x8	8x2
Frequency ($\omega_0/(2\pi)$)	33 kHz	32 kHz
Diffusion time (τ_{d})	0.46 µs	0.46 µs
Operation point ($\omega\tau_{\mathrm{d}}$)	0.095	0.092
$\frac{d}{dp} b_{squeeze}^{theory}$	$2.43 \cdot 10^{-6}$ kg/s/mbar	$0.61 \cdot 10^{-6}$ kg/s/mbar
$\frac{d}{dp} b_{squeeze}^{observed}$	$1.76 \cdot 10^{-6}$ kg/s/mbar	$0.87 \cdot 10^{-6}$ kg/s/mbar

This is not surprising due to the simplifications in the calculation of the effective diffusion time $\tau_{\mathrm{d,eff}}$. As yet, we have used $\tau_{\mathrm{d,eff}} = \tau_{\mathrm{d}}$, resulting in $\omega\tau_{\mathrm{d}}$ = 0.095 and 0.092 for the 8x8 and 8x2 device, respectively. Monte Carlo methods can be applied to calculate this number very accurately. This still has to be done: results will be presented at the conference.

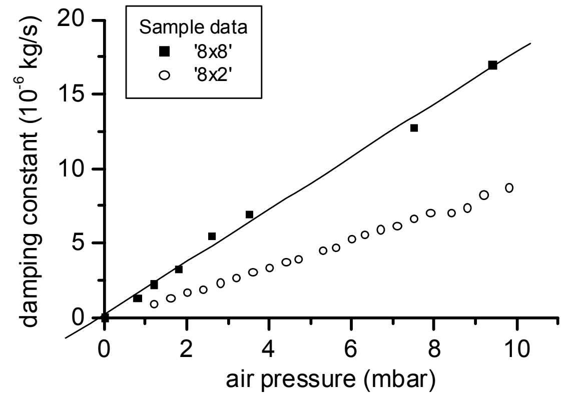

Figure 6: Air pressure dependency of the measured damping coefficients on two different MEMS resonators specified in fig. 4 and tab. 1. To guide the eye a straight line is fitted through the '8x8' sample data

7. Concluding remarks

We have introduced a fully analytical model for the damping of an oscillating plate in the regime of free molecular flow. This model is based in the well known properties of free molecular flow and the interaction of gas molecules with a surface at conditions that prevail in an environment that does resemble the operation of a MEMS in a package or a test chamber. Full thermal accommodation is the rule; specular reflection is the exception in all practical cases. Through the model we have gained insight which allows us to design tailor-made devices that will operate on specification.

8. References

1. M. Bao, H. Yang, H. Yin, Y. Sun, *J. Micromech. Microeng*. 12 (2002) 341–346.
2. J. Zook, D. Burns, H. Guckel, J. Sniegowski, R. Engelstad, Z. Feng, *Sens. Actuators A* 35 (1992) 51–59.